ARTICLE

One-pot synthesis of in situ carbon-decorated Cu$_3$P particles with enhanced electrocatalytic hydrogen evolution performance

Mingyu Pi
College of Physics, Chongqing University, Chongqing 401331, China

Tao Yang
College of Chemical Engineering, Chongqing University, Chongqing 401331, China

Shuxia Wang and Shijian Chen[a)]
College of Physics, Chongqing University, Chongqing 401331, China

Developing highly efficient and low-cost electrocatalysts with robust stability for hydrogen evolution reaction (HER) is a significant but challenging work for energy conversion and storage in recent years. In the present work, in situ carbon-decorated Cu$_3$P particles (Cu$_3$P@C) were facially synthesized by a one-pot rapid reaction with the precursors of copper acetylacetonate [Cu(acac)$_2$] and triphenylphosphine (PPh$_3$) at 425 °C for 1 h via a vacuum encapsulation technique. Compared with pure Cu$_3$P particles, the Cu$_3$P@C hybrid catalyst exhibits an enhanced electrocatalytic water-splitting performance for hydrogen evolution with excellent stability. The investigation shows that the hybridization with carbon efficiently facilies the charge transport for the electrochemical reaction. Such results of our study make the present Cu$_3$P@C-based hybrid a promising catalyst for practical applications toward energy conversion and pave way for designing and fast fabricating in situ carbon-decorated HER catalysts from the organometallic precursors.

I. INTRODUCTION

With the rapid consumption of fossil fuels for energy demands and increasing environment crisis, an urgent demand for clean energy sources have attracted a wide horizon of research interest over the past few years. Hydrogen has been considered an ideal and sustainable alternative source for fossil fuels for the human society owing to the highest possible energy density, renewable, and zero greenhouse gases emission properties.[1–3] Among the clean-energy developing methods, electrochemical splitting of water to produce hydrogen is a promising strategy due to its low energy consumption, short reaction period, high-purity product, and environmentally friendly process. However, such methods need to seek highly efficient hydrogen evolution reaction (HER) electrocatalysts that can provide a large mediation for the reaction at a low overpotential,[4–6] which represents a vital step to accelerate the development of hydrogen economy but remains challenging for now.[7]

Over the recent years, great efforts have been made to explore the high efficiency, low cost, and strong durability of nonprecious metal substitutes.[8–10] As yet, many nonprecious metals,[11,12] transition metal alloys,[13–16]

transition-metal carbides,[17–19] chalcogenides,[20–24] nitride,[25–27] oxide[28–30] and borides[31] have been widely investigated for their electrocatalytic HER properties. Even though a great deal of research work has been put in during the past few decades, the HER catalysts still face several challenging problems: (i) the catalytic performance of the most reported HER electrocatalysts are much lower than the Pt/C catalysts and need to be further promoted; (ii) some electrocatalysts that show good HER activities are still dependent on the assistance of noble metal materials; (iii) the hybrid catalysts with the combination of two or more phases cannot easily maintain their activities due to complicated components and structures; (iv) many electrocatalysts suffer from the bad stability toward HER. Recently, metal phosphides-based composites (MPCs), which are known as the alloy of phosphorus and a transition metal, showing metallic and submetallic properties (such as the high electron transfer and small or no band-gap energy)[32] have been discovered as excellent HER catalysts, such as Mo-, W-, Fe-, Co-, Ni-, and Cu-based phosphides.[33–38] Among these, Cu$_3$P is usually investigated as the electrode material for lithium-ion batteries in early articles.[39,40] Very recently, Sun and co-workers proposed the preparation of self-standing Cu$_3$P nanowire arrays on commercial porous copper foam as a monolithic high-efficient three-dimensional (3D) cathode for electrocatalytic hydrogen evolution with long-term stability.[41] Shen

and his group reported synthesis of Cu$_3$P nanocubes and developed it as an excellent catalyst for electrocatalytic hydrogen generation in acidic solution.[42] Chen et al. developed Cu$_3$P nanosheet as an efficient and robust bifunctional catalyst for electrocatalytic overall water splitting.[43] However, except for the above reports, the study of Cu$_3$P as an electrocatalyst for hydrogen evolution comprises only few studies up to now.

For catalysts of HER, besides chemical constituents and morphology characters, electric conductivity also plays an important role in their electrochemical performance.[44] Despite that most of the MPCs possess metallic and metalloid features, it is still necessary to increase the electronic conductivity for the catalysts by using the assisted method, because there are contact resistances between the catalytic active materials. Such strategies to fabricate the catalysts' nanostructure arrays on a carbon fiber cloth (e.g., the WP$_2$ nanowire arrays on carbon cloth as a 3D flexible electrode for efficient electrocatalytic hydrogen evolution)[45] or commercial porous metal foam (e.g., electrodeposition of Ni–P nanoparticles film on copper foam as a bifunctional electrocatalyst for water splitting to produce hydrogen)[46] are promising approaches to guarantee rapid electron transport for electrochemical reactions. In addition, hybridization with carbon is another efficient strategy to increase the conductivity of active materials. For example, Zhang et al. and Wang et al. reported carbon-coated Fe$_3$O$_4$ nanospindles[47] and nanorings[48] as electrode materials for lithium-ion batteries, respectively. Gao et al. reported the preparation of carbon-coated MoP nanoparticles as efficient hydrogen evolution electrocatalyst.[49] Compared with the counterpart without the carbon coating, all of them show an enhanced performance on account of the carbon decoration, which effectively increases the electron transport of the catalysts. At the same time, the carbon decoration of the catalyst can also protect the catalyst from corrosion of the electrolyte solution, which can further enhance the stability of the catalyst.

In this work, we report a facial one-pot synthesis strategy to prepare in situ carbon-decorated Cu$_3$P particles (Cu$_3$P@C) via rapid reaction of the precursors of copper acetylacetonate [Cu(acac)$_2$] and triphenylphosphine (PPh$_3$) at 425 °C for 1 h with the assistance of a vacuum system. As far as we know, this is the first time the Cu$_3$P@C hybrid has been synthesized in such a short reaction time under mild conditions. As a catalyst for electrochemical hydrogen evolution, the Cu$_3$P@C hybrid was investigated in the current work. Compared with pure Cu$_3$P particles, the Cu$_3$P@C hybrid shows an enhanced electrocatalytic performance for hydrogen evolution with excellent stability. It is evidenced that the in situ decoration of carbon efficiently facilities and ensures a fast electron transport for the electrochemical reaction. The results of our study make the present Cu$_3$P@C-based

hybrid a promising catalyst for practical applications toward energy conversion and pave a way for designing and fast fabricating in situ carbon-decorated HER catalysts from the organometallic reaction precursors.

II. EXPERIMENTAL SECTION

A. Materials

Copper acetylacetonate [Cu(acac)$_2$], copper (Cu) nanoparticles, and triphenylphosphine (PPh$_3$) were purchased from Alfa Aesar (Shanghai, China). Commercially available Pt/C (20%) catalyst and Nafion solution (5 wt%) were purchased from Shanghai Chemical Regent Company (Shanghai, China). The ethanol and toluene solvents were obtained from Adamas-beta (Shanghai, China). All the chemicals were used as received, without further purification. The deionized water used in our experiments was purified using a Millipore system (Millipore, Milli-Q Advantage A10, Shanghai, China).

B. Synthesis of Cu$_3$P@C-based hybrid catalyst

The Cu$_3$P@C-based hybrid catalyst was synthesized via one-pot liquid-phase phosphidation strategy with the assistance of a vacuum system. In a typical synthesis: 30 mg of Cu(acac)$_2$ and 180 mg of PPh$_3$ were uniformly mixed and encapsulated in a vacuum (~3 × 10^{-4} Pa) quartz tube. Afterward, the sealed tube was loaded into a muffle furnace, which was then heated from room temperature to 425 °C in 213 min, and kept at this reaction temperature for 1 h. After that, the tube was cooled down to room temperature naturally, the black products were collected from the silica tube, then the product was repeatedly washed by toluene and absolution ethanol with ultrasonic treatment, and finally dried at 60 °C in a vacuum oven for further investigation.

C. Synthesis of Cu$_3$P catalyst

For comparison, the Cu$_3$P nanoparticles without carbon decoration were also prepared by directly phosphating Cu nanoparticles using a similar phosphidation reaction process: 32 mg of Cu and 180 mg of PPh$_3$ were uniformly mixed and encapsulated in a vacuum (~3 × 10^{-4} Pa) quartz tube. Afterward, the sealed tube was loaded into a muffle furnace, which was then heated from room temperature to 400 °C in 200 min, and kept at this reaction temperature for 20 h. After that, the tube was cooled down to room temperature naturally, the black products were collected from the silica tube, the product was then repeatedly washed by using toluene and absolution ethanol with ultrasonic treatment, and finally dried at 60 °C in a vacuum oven for further investigation.

D. Characterizations

The purity and phase of the samples were identified using the X-ray diffractometer (XRD) data collected by

the powder XRD (Rigaku D/MAX2500PC, Rigaku Corporation, Beijing, China) with Cu K_α radiation (1.54178 Å). The field-emission scanning electron microscopy (FE-SEM, TESCAN MIRA 3, Boyue Instrument Ltd, Shanghai, China) was utilized for morphological and structure observation with an accelerating voltage of 25 kV, and the corresponding energy dispersive X-ray (EDX) spectrum of the samples were obtained by using a matched X-ray spectrometer for the FE-SEM. Measurements were also performed using the transmission electron microscopy (TEM; Hitachi, Tokyo, Japan) to further reveal the microstructure of the obtained products. The specific surface area was tested by using an automated surface area and pore size analyzer (Quadrasorb 2MP, Quantachrome Instruments, Boynton Beach, Florida). The Raman spectrums were taken under ambient conditions by using a Raman spectrometer (Labram HR 800 Raman, Horiba Corp, Shanghai, China). The X-ray photoelectron spectra (XPS) characterizations were performed on a Thermo ESCALAB 250Xi X-ray photoelectron spectrometer (Thermo Fisher Scientific, Waltham, Massachusetts) with Al K_α X-ray sources.

E. Electrochemical measurements

All the electrochemical characterizations were performed by using an electrochemical workstation (CHI 660E; CH Instruments, Shanghai, China) at room temperature in a typical three-electrode setup, and 0.5 M H_2SO_4 was utilized as the electrolyte solution. The graphite rod was used as the counter electrode, and saturated calomel electrode (SCE) was used as the reference electrode. A piece of carbon fiber paper (CFP) coated with the Cu₃P-based catalyst was used as the working electrode. The fabrication process for the working electrode is described as follows: 10 mg of the Cu₃P-based catalyst was dispersed in 500 μL of water–ethanol solution (with volume ratio of 300:190) containing 10 μL of 5 wt% Nafion solution by ultrasonic treatment for several hours to form a homogeneous ink. Afterward, a certain volume of the catalyst ink was loaded onto the CFP substrate (catalyst loading density ∼1 mg/cm²). Here, the CFP substrate was cleaned by repeat ultrasonic treatment for 10 min with deionized water, acetone, and ethanol solutions, respectively. The potential measured by the SCE reference electrode in our work was converted to potential against reversible hydrogen electrode (RHE) according to the equation: $E_{RHE} = E_{SCE} + 0.242 + 0.059$ pH, and the iR compensation was also applied to all initial data for further analysis. For linear sweep voltammetry (LSV) tests, the sweeping potential range is −0.6 to 0 V (versus RHE) in 0.5 M H_2SO_4, and the scan rate was set to be 2 mV/s. The electrochemical impedance spectroscopy (EIS) tests were measured at −0.1 V (versus RHE) within the frequency ranging from 100 kHz to 0.01 Hz. The cyclic voltammetric (CV) measurements were conducted from +0.1 to −0.3 V (versus RHE) at a scan rate of 100 mV per second. The time dependency response of catalytic current density during electrochemical reaction for the Cu₃P@C hybrid catalyst was carried out at a constant potential of 205 mV (versus RHE) after equilibrium.

III. RESULTS AND DISCUSSION

The approach of reacting organometallic precursors with PPh₃ in an evacuated and sealed silica tube has been confirmed as an efficient method to prepare the MPC catalytic materials. The high boiling point of PPh₃ makes it possible to synthesize MPC products via a solution-phased route during the reaction, and the graphitization of the carbon species from the organometallic sources can in situ decorate the MPCs.[50] In this work, by reacting Cu(acac)₂ with PPh₃ in the vacuum and encapsulated quartz tube, the Cu₃P@C hybrid was successfully synthesized. The reaction process schematic diagram of the Cu₃P@C product is shown in Fig. 1(a); the thermal decomposition of organometallic compound Cu(acac)₂ provided the carbon and copper sources while PPh₃ acted as the phosphorus source and reacted with the newly born copper species to produce the new type of transition-metal phosphide/carbon hybrid product, and the Cu₃P@C hybrid shows a specific surface area of 122 m²/g with a wide pore size distribution from 2 to 10 nm (Fig. S1). Additionally, the Cu₃P nanoparticles without the carbon decoration for the comparison were also prepared by directly phosphating Cu nanoparticles using the same phosphidation procedure. Cu₃P is a well-known form of copper phosphide, and Fig. 1(b) shows its crystal structure. Cu₃P crystallized in the hexagonal type with space group of $P6_3cm$, and the corresponding lattice constants are $a = 6.958$, $b = 6.958$, and $c = 7.178$ Å, respectively. The crystal structure and phase purity of the obtained Cu₃P@C and Cu₃P samples were characterized by powder XRD. The XRD patterns of the as-prepared products, as shown in Fig. 1(c), can be accurately indexed to the typical CuP₃ phase (JCPDS card no. 71-2261), indicating that the CuP₃-based catalysts are successfully prepared.

FE-SEM was used to observe the morphologies of the as-prepared samples. It can be seen from Figs. 2(a) and 2(b) that the sample consists of microparticles coated with sheet-like materials, and the TEM image [Fig. 2(c)] further reveals such hierarchical structure for the Cu₃P@C hybrid. Figure S2 shows the SEM and TEM images of pure Cu₃P, which indicates that the pure Cu₃P products are the nanoparticles with irregular morphology. EDX spectra of the sample in Fig. 2(d) demonstrates that it is composed of C, Cu, and P, and the atomic ratio for Cu and P is about 3.3:1, which is close to the expected stoichiometry for the Cu₃P. Furthermore, as shown in Fig. 2(e), the SEM image and the corresponding EDX elemental mapping images for the sample indicate that the Cu and P elements are evenly
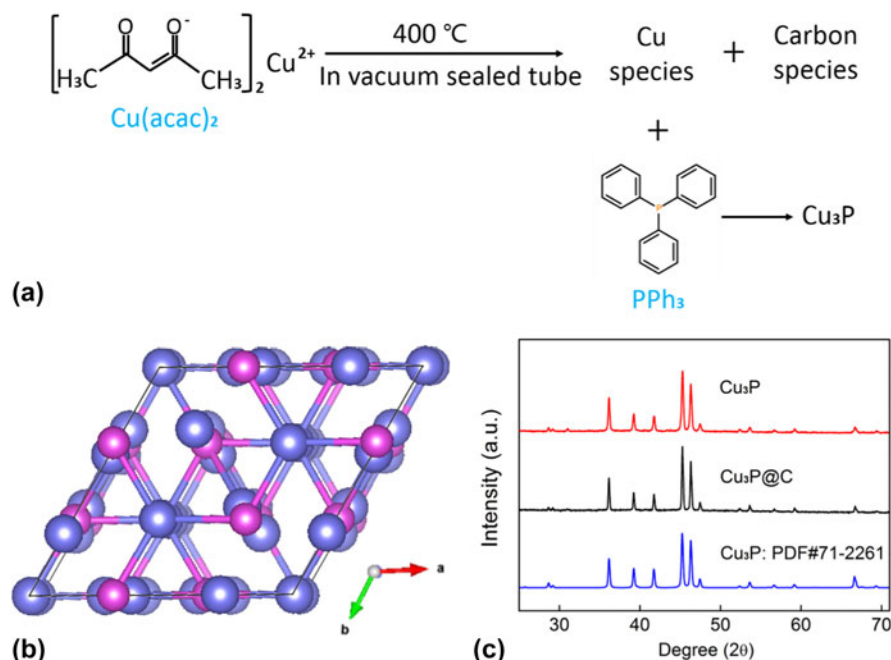
FIG. 1. (a) Synthesis process of the Cu₃P@C product. (b) Crystal structure of the Cu₃P (purple ball—copper atom, pink ball—phosphorus atom). (c) XRD patterns for the Cu₃P and Cu₃P@C samples.

distributed in the Cu₃P@C hybrid, and the carbon coats on them. In addition, the Raman spectra [Fig. 3(a)] of the Cu₃P@C sample shows two intensive peaks with wave numbers of 1346 and 1585 cm^{-1}. The D-band at about 1346 cm^{-1} is attributed to the vibration of carbon atoms with dangling bonds in the plane termination of disordered graphite, whereas the G-band at 1585 cm^{-1} is associated with the vibration of sp^2 hybridized carbon atoms in a graphite layer,[51] which further confirms the presence of carbon in the Cu₃P@C hybrid. The disorder degree of carbon is in proportion to the relative intensity ratio of the two bands (I_D/I_G), and the low I_D/I_G ratio implies the high graphitization of carbon, which can further promote the charge transfer for the electrochemical reaction.[26] However, there are no characteristic peaks of graphite for the pure Cu₃P nanoparticles. All of the above results strongly verify the successful preparation of carbon-decorated Cu₃P particles.

To further explore the chemical composition of the prepared Cu₃P@C hybrid, the XPS test was performed. Figure 3(b) shows the XPS survey spectra, and the Cu₃P@C sample can be obtained that only contains P, Cu, C, and O. The signal of O could be originated from the adsorbed oxygen, oxygen-containing groups, and surface oxidation of the sample in air. The strong peak of C also confirms the existence of carbon in the Cu₃P@C hybrid. Figures 3(c) and 3(d) show the magnified close-up and fitted spectra in the P and Cu regions for the Cu₃P@C hybrid, respectively. As shown in Fig. 3(c), the P 2p region shows two peaks at 129.6 and 130.3 eV, reflecting the binding energy (BE) of P 2p$_{3/2}$ and P 2p$_{1/2}$,

respectively. The primary P 2p$_{3/2}$ at 129.6 eV comes from the P–Cu bond. Here, the peak at 134.2 eV can be attributed to the oxidization of P species as a result of air contact. In the Cu region [Fig. 3(d)], the peak at the BE of 932.9 and 952.7 eV are indexed to Cu 2p$_{3/2}$ and Cu 2p$_{3/1}$, respectively. According to an early report, both of the hydrogenase and metal complex toward HER combine proton relays from pendant acid–base groups near the metal center.[52,53] For WP₂[54,55] and MoP₂[56] hydrogen evolution electrocatalyst, they are also characterized by pendant base P (δ^-) near the metal center M (δ^+). For elements Cu and P, the BEs are 932.6 eV and 130.2 eV,[57] respectively, therefore the BE of P 2p$_{3/2}$ shifts to low energy and that of Cu 2p$_{3/2}$ exhibits a positive shift, indicating that the P site has a partial negative charge (δ^-) and the Cu site has a partial positive charge (δ^+) in the Cu₃P@C hybrid catalyst, then the electron density will have a small transfer from Cu to P, which is the ligand effect,[58,59] and it is desirable for an excellent performance HER electrocatalyst. On the base of the above XPS analysts, it can be deduced that the Cu₃P catalyst may follow a similar catalytic reaction principle toward hydrogen evolution with hydrogenase, metal complex, and other transition-metal phosphide electrocatalysts.

The HER catalytic performances of the Cu₃P and Cu₃P@C catalysts with the same loading were evaluated using a three-electrode electrochemical workstation with the electrolyte solution of 0.5 M H₂SO₄. The commercially available Pt/C catalyst and bare CFP substrate were also examined for comparison. Figure 4(a) shows the LSV polarization curves for Pt/C, bare CFP, Cu₃P, and
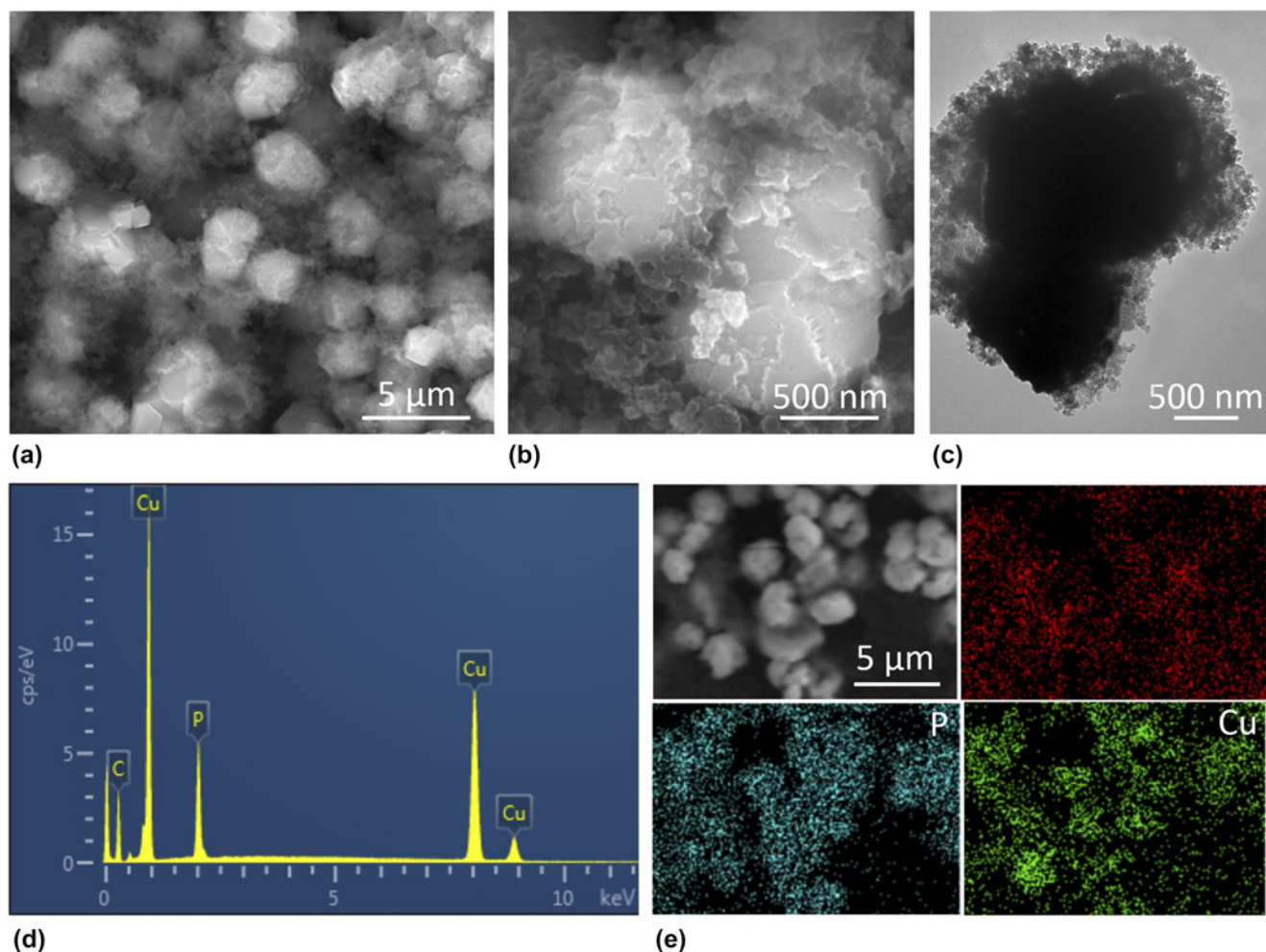
J. Mater. Res., Vol. 33, No. 5, Mar 14, 2018

549

FIG. 2. (a) Scanning electron microscopy (SEM), (b) magnified SEM, and (c) TEM images for the Cu$_3$P@C hybrid sample. (d) EDX spectra and (e) SEM image and the corresponding EDX elemental mappings of C (red), P (blue), and Cu (green) for the Cu$_3$P@C hybrid sample.

Cu$_3$P@C hybrid. It is found that the Pt/C catalyst exhibits super excellent HER activity with a near-zero overpotential, whereas the bare CFP substrate shows a rather poor activity with negligible current density. The pure Cu$_3$P particles exhibit fairly good activities. As observed, to achieve the cathodic current density of 10 mA/cm^2, it needs overpotential of 263 mV for the pure Cu$_3$P catalyst. However, it is notable that when using the Cu$_3$P@C hybrid catalyst, the electrocatalytic activities were dramatically improved, and it only requires overpotential of 203 mV to drive the same current density, which can compare favorably with the performances of other reported Cu$_3$P catalysts (Table S1). It is well known that Tafel slop is another important factor utilized to further get an insight into the electrocatalytic activity toward HER. A smaller Tafel slop indicates a better HER performance which leads to an enhanced HER rate with an increase in overpotential. Figure 4(b) shows the Tafel plots for the Pt/C, Cu$_3$P, and Cu$_3$P@C hybrid, respectively. These linear portions are fitted to the Tafel

equation [η versus log (current density) and η is the overpotential]. The Tafel slope of 31 mV/dec for Pt/C catalyst is consistent with the reported value.[41] The value of Tafel slop for the pure Cu$_3$P catalyst is calculated to be 91 mV/dec. However, when using the Cu$_3$P@C hybrid catalyst, this value decreases to 83 mV/dec, which suggests that the Cu$_3$P@C hybrid catalyst possesses a superior catalytic activity toward HER over the pure Cu$_3$P catalyst, and base on the early report,[41] it can also be obtained that the HER for the both catalysts follows a Volmer-Heyrovsky mechanism [Fig. 4(c)], wherein the electrolytic reaction is limited by the electrochemical desorption step. Besides, by using the extrapolation method to the Tafel plot, the exchange current density of the Cu$_3$P@C hybrid catalyst is calculated to be 0.025 mA/cm^2, which is about twice that of the pure Cu$_3$P catalyst (0.013 mA/cm^2), highlighting the enhanced H$_2$ evolving efficiency for the Cu$_3$P@C hybrid catalyst.

As an important evaluation for an electrocatalyst, the stability of the polarization curves was also characterized
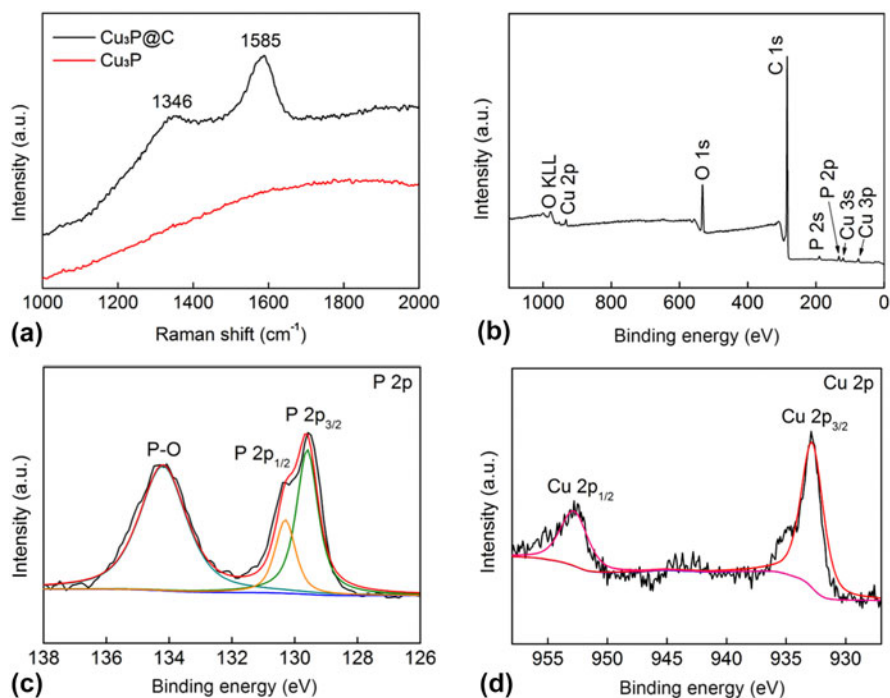
FIG. 3. (a) Raman spectrums for the Cu$_3$P and Cu$_3$P@C hybrid. (b) XPS survey spectrum for the Cu$_3$P@C hybrid. XPS spectra in the P 2p (c) and Cu 2p (d) regions for the Cu$_3$P@C hybrid.
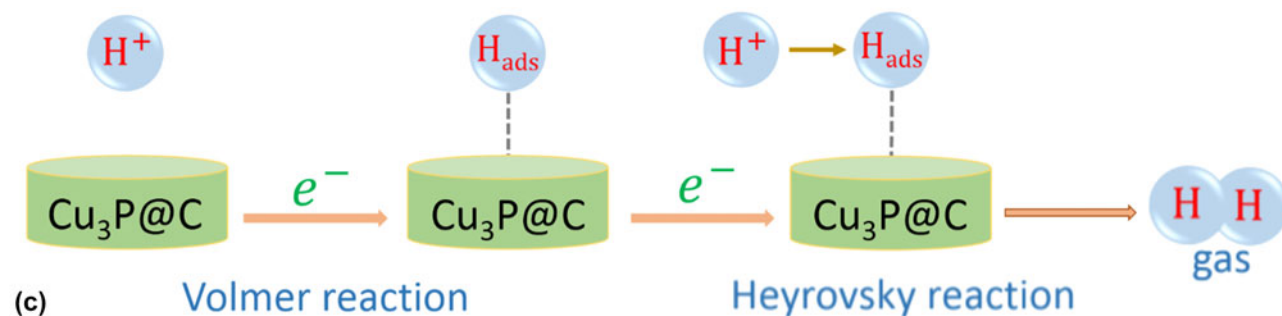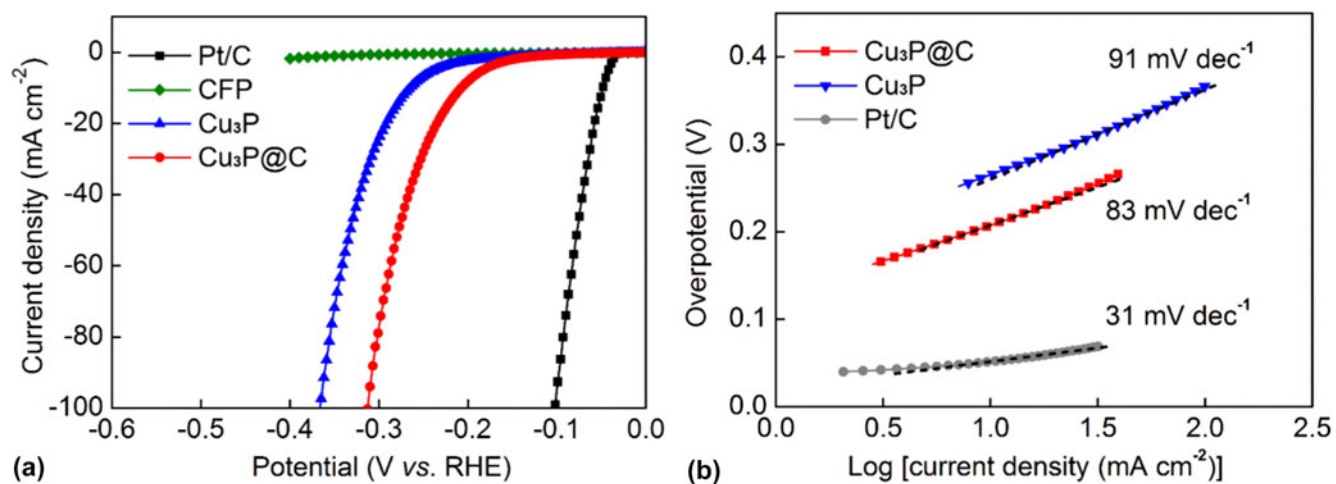

FIG. 4. (a) Polarization curves for the Pt/C, bare CFP, Cu$_3$P, and Cu$_3$P@C hybrid catalyst in 0.5 M H$_2$SO$_4$ with a scan rate of 2 mV/s. (b) Tafel plots for the Pt/C, Cu$_3$P, and Cu$_3$P@C. (c) HER catalytic process undergoes a Volmer–Heyrovsky mechanism for the Cu$_3$P@C hybrid catalyst.
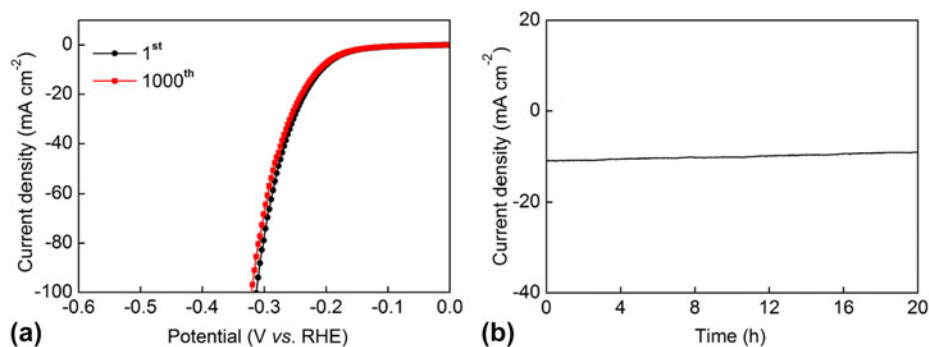
FIG. 5. (a) Polarization curves for the Cu₃P@C hybrid catalyst initial and after 1000 CV scanning between +0.1 and −0.3 V with a scan rate of 100 mV/s. (b) Current density versus time curve for the Cu₃P@C hybrid catalyst for 20 h under the static potential of 205 mV.
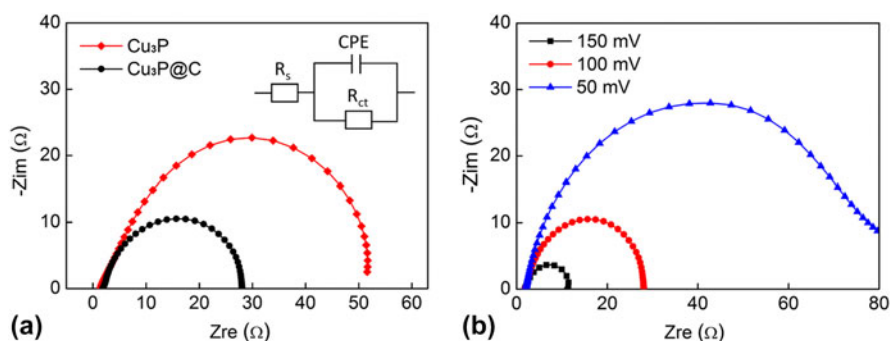

FIG. 6. (a) Nyquist plots and data fitting to a simplified circuit for the Cu₃P and Cu₃P@C. (b) Nyquist plots for the Cu₃P@C hybrid under different overpotentials.

by attenuation tests and constant overpotential measurements for the Cu₃P@C hybrid catalyst. Figure 5(a) shows the attenuation tests that were performed by 1000-times cyclic sweep for the catalytic materials in 0.5 M H₂SO₄ between +0.1 and −0.3 V (versus RHE) with a certain scan rate of 100 mV/s. From the CV curves, we can see that the final polarization curve of the Cu₃P@C hybrid catalyst nearly overlaps with the first one. To achieve the current density of 10 mA/cm², the overpotential only increased 5 mV for the Cu₃P@C hybrid catalyst after the CV scanning of 1000 times, which shows the excellent stability of the catalyst. The catalytic stability of the Cu₃P@C hybrid was further characterized by conducting constant overpotential response tests of the current density at 205 mV (versus RHE). As shown in Fig. 5(b), the responded current density for the Cu₃P@C hybrid catalyst has a minor decrease after a long test period of 20 h. Here, the minor decrease may be attributed to the fact that the protons in the electrolyte solution suffer depletion and that the generated gas bubbles adsorbed on the surface of the working electrode hinder the electrolytic reaction. All of the above results confirm the robust catalytic stability toward HER for the prepared Cu₃P@C hybrid catalyst.

To examine the electrode kinetics and further reveal the superior HER performance of the Cu₃P@C hybrid

catalyst, the EIS test was performed. The corresponding Nyquist plots and data fitting to a simplified circuit are shown in Fig. 6(a). As observed, the Niquist plots of both catalysts possess a semicircular shape. As we know, the radius of the semicircle can serve as the reflection of the charge transfer resistance (R_{ct}) or Faraday interfacial resistance for the electrode. The Cu₃P@C hybrid catalyst exhibits a R_{ct} for the reduction of protons at the electrolyte/catalyst interface of approximately 26 Ω, which is much smaller than that of the pure Cu₃P catalyst (50 Ω), indicating a better electron transfer, and also confirming that the decoration of carbon for the catalyst dramatically enhances the electronic conductivity, which consequently increases the catalytic activities of the catalyst. In addition, the low series resistance (about 2 Ω) indicates the effective electrical integration with small ohmic losses between the catalysts and the conductive substrate. Furthermore, the Nyquist plots for the Cu₃P@C catalyst were also recorded at different overpotentials [Fig. 6(b)]. As expected, the R_{ct} sharply decreases with the increasing overpotential, and this is well agreed with the tendency of HER polarization curve, which reveals the potential dependency nature of the Cu₃P@C hybrid catalyst.

Overall, such enhanced HER catalytic activity of the Cu₃P@C hybrid catalyst can be mainly ascribed to the

following aspects: (i) the catalyst consists of Cu_3P, known as highly active catalyst toward water splitting for hydrogen evolution; (ii) as shown in Fig. S3, the electrons transfer from the CFP substrate to carbon nanosheets and then transfer to the surface of Cu_3P particles to conduct the reduction of protons to produce hydrogen. Therefore the decoration of carbon efficiently increases the electron transport for the Cu_3P particles catalyst, which consequently improves the electrocatalytic performance toward hydrogen evolution; (iii) the low I_D/I_G ratio in the Raman spectrum implies that the carbon in a $Cu_3P@C$ hybrid has a high graphitization, comparing with the carbon with low graphitization, it can provide more enhancement for the charge transfer of the catalyst during the electrochemical reaction; (iv) the Cu_3P particles are well dispersed in the graphitic carbon matrix leading to the hierarchical structure of the $Cu_3P@C$ hybrid catalyst consisting of microparticles with coated sheet-like structure, which may bring in large surface area to expose luxuriant active sites and may also favor H^+ absorption on the surface of the catalyst during the electrochemical reaction.

IV. CONCLUSIONS

In this work, we proposed a facial and rapid method to synthesize in situ carbon-decorated Cu_3P ($Cu_3P@C$) via a one-pot reaction of the precursors of copper acetylacetonate $[Cu(acac)_2]$ and triphenylphosphine (PPh_3) at 425 °C for 1 h with the assistance of vacuum encapsulation technique. Compared with the pure Cu_3P catalyst, the $Cu_3P@C$ hybrid exhibits an enhanced electrocatalytic water-splitting performance for hydrogen evolution with excellent stability. For the $Cu_3P@C$ hybrid catalyst, the enhanced HER catalytic activities were also explored. Such results of our study provide an opportunity for the present $Cu_3P@C$-based hybrid as an excellent electrocatalyst for water splitting toward energy conversion and pave a way for designing and fast fabricating in situ carbon-decorated HER catalysts from the organometallic reaction precursors.

ACKNOWLEDGMENTS

REFERENCES

1. J. Chow, R.J. Kopp, and P.R. Portney: Energy resources and global development. *Science* **302**, 1528 (2003).
2. W. Zhang, W.Z. Lai, and R. Cao: Energy-related small molecule activation reactions: Oxygen reduction and hydrogen and oxygen evolution reactions catalyzed by porphyrin- and corrole-based systems. *Chem. Rev.* **111**, 3717 (2017).
3. X. Li, J.G. Yu, J.X. Low, Y.P. Fang, J. Xiao, and X.B. Chen: Engineering heterogeneous semiconductors for solar water splitting. *J. Mater. Chem. A* **3**, 2485 (2015).
4. X.Z. Wang, H. Zhou, P. Li, and W.M. Shu: Vertically aligned carbon nanotube-based electrodes for hydrogen production by water electrolysis. *J. Mater. Res.* **28**, 927 (2013).
5. M. Blouin, D. Guay, J. Huot, and R. Schulz: High energy ball-milled Ti₂RuFe electrocatalyst for hydrogen evolution in the chlorate industry. *J. Mater. Res.* **12**, 1492 (1997).
6. J.H. Wang, W. Cui, Q. Liu, Z.C. Xing, A.M. Asiri, and X.P. Sun: Recent progress in cobalt-based heterogeneous catalysts for electrochemical water splitting. *Adv. Mater.* **28**, 215 (2016).
7. Y.M. Shi and B. Zhang: Recent advances in transition metal phosphide nanomaterials: Synthesis and applications in hydrogen evolution reaction. *Chem. Soc. Rev.* **45**, 1529 (2016).
8. Y.Z. Han, H.Y. Fang, H.Z. Jing, H.L. Sun, H.T. Lei, W.Z. Lai, and R. Cao: Singly versus doubly reduced nickel porphyrins for proton reduction: Experimental and theoretical evidence for a homolytic hydrogen-evolution reaction. *Angew. Chem., Int. Ed.* **55**, 5457 (2016).
9. J.R. McKone, E.L. Warren, M.J. Bierman, S.W. Boettcher, B.S. Brunschwig, N.S. Lewis, and H.B. Gray: Evaluation of Pt, Ni, and Ni–Mo electrocatalysts for hydrogen evolution on crystalline Si electrodes. *Energy Environ. Sci.* **4**, 3573 (2011).
10. S.C. Lin, Y.F. Chiu, P.W. Wu, Y.F. Hsieh, and C.Y. Wu: Templated fabrication of nanostructured Ni brush for hydrogen evolution reaction. *J. Mater. Res.* **25**, 2001 (2010).
11. L.L. Fan, P.F. Liu, X.C. Yan, L. Gu, Z.Z. Yang, H.G. Yang, S.L. Qiu, and X.D. Yao: Atomically isolated nickel species anchored on graphitized carbon for efficient hydrogen evolution electrocatalysis. *Nat. Commun.* **7**, 10667 (2016).
12. B.R. Liu, L. Zhang, W.L. Xiong, and M.M. Ma: Cobalt-nanocrystal-assembled hollow nanoparticles for electrocatalytic hydrogen generation from neutral-pH water. *Angew. Chem., Int. Ed.* **55**, 6725 (2016).
13. Q. Lu, G.S. Hutchings, W.T. Yu, Y. Zhou, R.V. Forest, R.Z. Tao, J. Rosen, B.T. Yonemoto, Z.Y. Cao, H.M. Zheng, J.Q. Xiao, F. Jiao, and J.G. Chen: Highly porous non-precious bimetallic electrocatalysts for efficient hydrogen evolution. *Nat. Commun.* **6**, 6567 (2015).
14. X. Zhang, H.M. Xu, X.X. Li, Y.Y. Li, T.B. Yang, and Y.Y. Liang: Facile synthesis of nickel-iron/nanocarbon hybrids as advanced electrocatalysts for efficient water splitting. *ACS Catal.* **6**, 580 (2016).
15. H.B. Zhang, Z.J. Ma, J.J. Duan, H.M. Liu, G.G. Liu, T. Wang, K. Chang, M. Li, L. Shi, X.G. Meng, K.C. Wu, and J.H. Ye: Active sites implanted carbon cages in core–shell architecture: Highly active and durable electrocatalyst for hydrogen evolution reaction. *ACS Nano* **10**, 684 (2016).
16. M. Zeng, Y.L. Liu, F.P. Zhao, K.Q. Nie, N. Han, X.X. Wang, W.J. Huang, X.N. Song, J. Zhong, and Y.G. Li: Metallic cobalt nanoparticles encapsulated in nitrogen-enriched graphene shells: Its bifunctional electrocatalysis and application in zinc-air batteries. *Adv. Funct. Mater.* **26**, 4397 (2016).
17. J.S. Li, Y. Wang, C.H. Liu, S.L. Li, Y.G. Wang, L.Z. Dong, Z.H. Dai, Y.F. Li, and Y.Q. Lan: Coupled molybdenum carbide and reduced graphene oxide electrocatalysts for efficient hydrogen evolution. *Nat. Commun.* **7**, 11204 (2016).
18. X.J. Yang, X.J. Feng, H.Q. Tan, H.Y. Zang, X.L. Wang, Y.H. Wang, E.B. Wang, and Y.G. Li: N-doped graphene-coated molybdenum carbide nanoparticles as highly efficient electrocatalysts

for the hydrogen evolution reaction. *J. Mater. Chem. A* **4**, 3947 (2016).

19. Q.F. Gong, Y. Wang, Q. Hu, J.G. Zhou, R.F. Feng, P.N. Duchesne, P. Zhang, F.J. Chen, N. Han, Y.F. Li, C.H. Jin, Y.G. Li, and S.T. Lee: Ultrasmall and phase-pure W₂C nanoparticles for efficient electrocatalytic and photoelectrochemical hydrogen evolution. *Nat. Commun.* **7**, 13216 (2016).

20. K. Chang, X. Hai, H. Pang, H.B. Zhang, L. Shi, G.G. Liu, H.M. Liu, G.X. Zhao, M. Li, and J.H. Ye: Targeted synthesis of 2H- and 1T-phase MoS₂ monolayers for catalytic hydrogen evolution. *Adv. Mater.* **28**, 10033 (2016).

21. J. Deng, H.B. Li, J.P. Xiao, Y.C. Tu, D.H. Deng, H.X. Yang, H.F. Tian, J. Li, P.J. Ren, and X.H. Bao: Triggering the electrocatalytic hydrogen evolution activity of the inert two-dimensional MoS₂ surface via single-atom metal doping. *Energy Environ. Sci.* **8**, 1594 (2015).

22. P.D. Tran, S.Y. Chiam, P.P. Boix, Y. Ren, S.S. Pramana, J. Fize, V. Artero, and J. Barber: Novel cobalt/nickel–tungsten-sulfide catalysts for electrocatalytic hydrogen generation from water. *Energy Environ. Sci.* **6**, 2452 (2013).

23. P.D. Tran, T.V. Tran, M. Orio, S. Torelli, Q.D. Truong, K. Nayuki, Y. Sasaki, S.Y. Chiam, R. Yi, I. Honma, J. Barber, and V. Artero: Coordination polymer structure and revisited hydrogen evolution catalytic mechanism for amorphous molybdenum sulfide. *Nat. Mater.* **15**, 640 (2016).

24. X.Y. Yu, Y. Feng, Y. Jeon, B.Y. Guan, and X.W. Lou: Formation of Ni–Co–MoS₂ nanoboxes with enhanced electrocatalytic activity for hydrogen evolution. *Adv. Mater.* **28**, 9006 (2016).

25. H.J. Yan, C.G. Tian, L. Wang, A.P. Wu, M.C. Meng, L. Zhao, and H.G. Fu: Phosphorus-modified tungsten nitride/reduced graphene oxide as a high-performance, non-noble-metal electrocatalyst for the hydrogen evolution reaction. *Angew. Chem., Int. Ed.* **54**, 6325 (2015).

26. M.X. Chen, J. Qi, D.Y. Guo, H.T. Lei, W. Zhang, and R. Cao: Facile synthesis of sponge-like Ni₃N/NC for electrocatalytic water oxidation. *Chem. Commun.* **53**, 9566 (2017).

27. Y. Zhang, Y. Xie, Y.T. Zhou, X.W. Wang, and K. Pan: Well dispersed Fe₂N nanoparticles on surface of nitrogen-doped reduced graphite oxide for highly efficient electrochemical hydrogen evolution. *J. Mater. Res.* **32**, 1770 (2017).

28. X.D. Yan, L.H. Tian, M. He, and X.B. Chen: Three-dimensional crystalline/amorphous Co/Co₃O₄ core/shell nanosheets as efficient electrocatalysts for the hydrogen evolution reaction. *Nano Lett.* **15**, 6015 (2015).

29. Y.H. Li, P.F. Liu, L.F. Pan, H.F. Wang, Z.Z. Yang, L.R. Zheng, P. Hu, H.J. Zhao, L. Gu, and H.G. Yang: Local atomic structure modulations activate metal oxide as electrocatalyst for hydrogen evolution in acidic water. *Nat. Commun.* **6**, 8064 (2015).

30. R. Wu, J.F. Zhang, Y.M. Shi, D.L. Liu, and B. Zhang: Metallic WO₂–carbon mesoporous nanowires as highly efficient electrocatalysts for hydrogen evolution reaction. *J. Am. Chem. Soc.* **137**, 6983 (2015).

31. J. Masa, P. Weide, D. Peerers, I. Sinev, W. Xia, Z.Y. Sun, C. Somsen, M. Muhler, and W. Schuhmann: Amorphous cobalt boride (Co₂B) as a highly efficient nonprecious catalyst for electrochemical water splitting: Oxygen and hydrogen evolution. *Adv. Energy Mater.* **6**, 1502313 (2016).

32. M.Y. Pi, T.L. Wu, D.K. Zhang, S.J. Chen, and S.X. Wang: Facile preparation of semimetallic WP₂ as a novel photocatalyst with high photoactivity. *RSC Adv.* **6**, 15724 (2016).

33. L.H. Tian, X.D. Yan, X.J. Chen, L. Liu, and X.B. Chen: One-pot, large-scale, simple synthesis of CoₓP nanocatalysts for electrochemical hydrogen evolution. *J. Mater. Chem. A* **4**, 13011 (2016).

34. X.D. Wang, Y.F. Xu, H.S. Rao, W.J. Xu, H.Y. Chen, W.X. Zhang, D.B. Kuang, and C.Y. Su: Novel porous molybde-

num tungsten phosphide hybrid nanosheets on carbon cloth for efficient hydrogen evolution. *Energy Environ. Sci.* **9**, 1468 (2016).

35. L.H. Tian, X.D. Yan, and X.B. Chen: Electrochemical activity of iron phosphide nanoparticles in hydrogen evolution reaction. *ACS Catal.* **6**, 5441 (2016).

36. D. Zhou, L.B. He, W.X. Zhu, X.D. Hou, K.Y. Wang, G. Du, C.B. Zheng, X.P. Sun, and A.M. Asirid: Interconnected urchin-like cobalt phosphide microspheres film for highly efficient electrochemical hydrogen evolution in both acidic and basic media. *J. Mater. Chem. A* **4**, 10114 (2016).

37. A.B. Laursen, K.R. Patraju, M.J. Whitaker, M. Retuerto, T. Sarkar, N. Yao, K.V. Ramanujachary, M. Greenblatt, and G.C. Dismukes: Nanocrystalline Ni₅P₄: A hydrogen evolution electrocatalyst of exceptional efficiency in both alkaline and acidic media. *Energy Environ. Sci.* **8**, 1027 (2015).

38. A. Han, H.Y. Zhang, R.H. Yuan, H.X. Ji, and P.W. Du: Crystalline copper phosphide nanosheets as an efficient Janus catalyst for overall water splitting. *ACS Appl. Mater. Interfaces* **9**, 2240 (2017).

39. S.B. Ni, J.J. Ma, X.H. Lv, X.L. Yang, and L.L. Zhang: The fine electrochemical performance of porous Cu₃P/Cu and the high energy density of Cu₃P as anode for Li-ion batteries. *J. Mater. Chem.* **2**, 20506 (2014).

40. A.J. Zhou, B. Yang, W.H. Wang, X.Y. Dai, M.J. Zhao, J. Xue, M.G. Han, C. Fan, and J.Z. Li: Enhanced reversibility and electrochemical performances of mechanically alloyed Cu₃P achieved by Fe addition. *RSC Adv.* **6**, 26800 (2016).

41. J.Q. Tian, Q. Liu, N.Y. Cheng, A.M. Asiri, and X.P. Sun: Self-supported Cu₃P nanowire arrays as an integrated high-performance three-dimensional cathode for generating hydrogen from water. *Angew. Chem., Int. Ed.* **53**, 9577 (2014).

42. L.B. Ma, X.P. Shen, H. Zhou, J. Zhu, C.Y. Xi, Z.Y. Ji, and L.R. Kong: Synthesis of Cu₃P nanocubes and their excellent electrocatalytic efficiency for the hydrogen evolution reaction in acidic solution. *RSC Adv.* **6**, 9672 (2016).

43. C.C. Hou, Q.Q. Chen, C.J. Wang, F. Liang, Z.H. Lin, W.F. Fu, and Y. Chen: Self-supported cedarlike semimetallic Cu₃P nanoarrays as a 3D high-performance Janus electrode for both oxygen and hydrogen evolution under basic conditions. *ACS Appl. Mater. Interfaces* **8**, 23037 (2016).

44. Z. Xing, Q. Liu, A.M. Asiri, and X.P. Sun: Closely interconnected network of molybdenum phosphide nanoparticles: A highly efficient electrocatalyst for generating hydrogen from water. *Adv. Mater.* **26**, 5702 (2014).

45. M.Y. Pi, T.L. Wu, D.K. Zhang, S.J. Chen, and S.X. Wang: Self-supported three-dimensional mesoporous semimetallic WP₂ nanowire arrays on carbon cloth as a flexible cathode for efficient hydrogen evolution. *Nanoscale* **8**, 19779 (2016).

46. Q. Liu, S. Gu, and C.M. Li: Electrodeposition of nickel–phosphorus nanoparticles film as a Janus electrocatalyst for electro-splitting of water. *J. Power Sources* **299**, 342 (2015).

47. W.M. Zhang, X.L. Wu, J.S. Hu, Y.G. Guo, and L.J. Wan: Carbon coated Fe₃O₄ nanospindles as a superior anode material for lithium-ion batteries. *Adv. Funct. Mater.* **18**, 3941 (2008).

48. L. Wang, J. Liang, Y. Zhu, T. Mei, X. Zhang, Q. Yang, and Y. Qian: Synthesis of Fe₃O₄@C core–shell nanorings and their enhanced electrochemical performance for lithium-ion batteries. *Nanoscale* **53**, 627 (2013).

49. S. Gao, Y.P. Liu, G.D. Li, Y.C. Guo, Y.C. Zou, and X.X. Zou: General urea-assisted synthesis of carbon-coated metal phosphide nanoparticles for efficient hydrogen evolution electrocatalysis. *Electrochim. Acta* **199**, 99 (2016).

50. J. Jiang, C.D. Wang, W. Li, and Q. Yang: One-pot synthesis of carbon-coated Ni₅P₄ nanoparticles and CoP nanorods for high-rate and high-stability lithium-ion batteries. *J. Mater. Chem. A* **3**, 23345 (2015).

51. C. Lee, X. Wei, J.W. Kysar, and J. Hone: Measurement of the elastic properties and intrinsic strength of monolayer graphene. *Science* **321**, 385 (2008).

52. A.D. Wilson, R.K. Shoemaker, A. Miedaner, J.T. Muckerman, D.L. Dubois, and M.R. Dubois: Nature of hydrogen interactions with Ni(II) complexes containing cyclic phosphine ligands with pendant nitrogen bases. *Proc. Natl. Acad. Sci. U. S. A.* **104**, 6951 (2007).

53. H.L. Sun, Y.Z. Han, H.T. Lei, M.X. Chen, and R. Cao: Cobalt corroles with phosphonic acid pendants as catalysts for oxygen and hydrogen evolution from neutral aqueous solution. *Chem. Commun.* **53**, 6195 (2017).

54. M.Y. Pi, T.L. Wu, D.K. Zhang, S.J. Chen, and S.X. Wang: Phase-controlled synthesis and comparative study of α- and β-WP₂ submicron particles as efficient electrocatalysts for hydrogen evolution. *Electrochim. Acta* **216**, 304 (2016).

55. M.Y. Pi, T.L. Wu, W.M. Guo, X.D. Wang, D.K. Zhang, S.X. Wang, and S.J. Chen: Phase-controlled synthesis of polymorphic tungsten diphosphide with hybridization of monoclinic and orthorhombic phases as a novel electrocatalyst for efficient hydrogen evolution. *J. Power Sources* **349**, 138 (2017).

56. W.X. Zhu, C. Tang, D.N. Liu, J.L. Wang, A.M. Asiric, and X.P. Sun: A self-standing nanoporous MoP₂ nanosheet array: An advanced pH-universal catalytic electrode for the hydrogen evolution reaction. *J. Mater. Chem. A* **4**, 7169 (2016).

57. J.F. Moulder, J. Chastain, and R.C. King: *Handbook of X-ray Photoelectron Spectroscopy: A Reference Book of Standard Spectra for Identification and Interpretation of XPS Data* (Perkin-Elmer, Eden Prairie, MN, 1992).

58. Z.H. Pu, Q. Liu, A.M. Asiri, and X.P. Sun: Tungsten phosphide nanorod arrays directly grown on carbon cloth: A highly efficient and stable hydrogen evolution cathode at all pH values. *ACS Appl. Mater. Interfaces* **6**, 21874 (2014).

59. M.X. Chen, J. Qi, W. Zhang, and R. Cao: Electrosynthesis of NiP$_x$ nanospheres for electrocatalytic hydrogen evolution from a neutral aqueous solution. *Chem. Commun.* **53**, 5507 (2017).

Supplementary Material

To view supplementary material for this article, please visit https://doi.org/10.1557/jmr.2017.401.